

Time dependence of cisplatin-induced duplex dissociation of 15-mer RNAs and mature miR-146a†

Christopher Polonyi and Sofi K. C. Elmroth*

Cite this: *Dalton Trans.*, 2013, **42**, 14959

Received 3rd July 2013,

Accepted 22nd August 2013

DOI: 10.1039/c3dt51788h

www.rsc.org/dalton

The kinetics for the binding of cisplatin to duplex RNAs, two fully complementary model systems and mature miR-146a, exhibits a linear dependence on cisplatin concentration and results in duplex dissociation at 38 °C.

Our knowledge regarding the use of small non-coding RNAs (ncRNAs) as regulators of gene expression is currently under rapid expansion.¹ Various types of both single- and double-stranded RNAs have been identified today, ranging from the relatively short *ca.* 20-mer duplexes of mature microRNAs (miRs), to the much longer transcripts of *e.g.* long and circular non-coding RNAs (lncRNAs and circRNAs).^{2,3} A common feature of all these seems to be their involvement in the cellular machinery as regulators, and a role in fine-tuning protein production as their main function through interaction with the RNA induced silencing complex (RISC).^{4–6} In the developing human cell, the proper functioning of ncRNAs is known to be crucial for key events such as early differentiation and organ development.⁷ Consequently, dysregulation of ncRNAs is recognized today as a reliable signature feature of many common diseases, with diabetes and cancer as well documented examples.^{8–11}

In the case of cancer, clinically used treatment regimens involve the use of several different types of drugs, often including alkylating ones, *i.e.* molecules able to covalently modify nucleic acids. Here, the use of *cis*-Pt(NH₃)₂Cl₂ (cisplatin, **1**) has been particularly successful for the treatment of testicular cancer, with well documented efficacy also against other types, *e.g.* ovarian- and head-and-neck cancers.¹² With respect to the intracellular mode of action, the reaction path involving the binding of cisplatin to nuclear DNA – with induction of

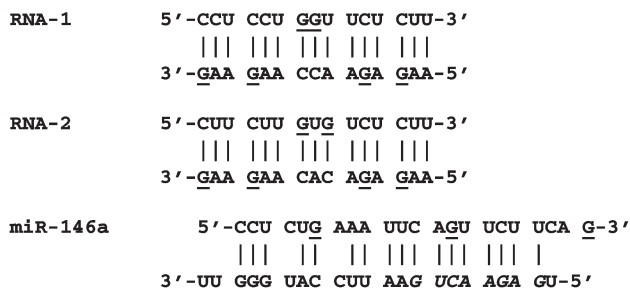
apoptosis and necrosis as downstream biological consequences – has so far been subjected to the most thorough investigations.¹³ However, since the ncRNAs are already present in the cytosol, where activation of cisplatin by formation of the corresponding monoquo complex *cis*-[Pt(NH₃)₂Cl(OH₂)]⁺ (**1a**) takes place, RNA binding is also prone to occur.^{14–18} To address the latter phenomenon, our laboratory has initiated research aiming at investigating the ability of platinum-based drugs to interfere with the RISC function.^{4,6,19,20} We have previously been able to show that fully complementary RNAs (siRNAs) processed by RISC maintained their function after platination,^{21–23} but with a typical overall trend of a moderately reduced silencing ability when compared to their corresponding unplatinated siRNAs. Due to the multistep process leading to silencing, the origin of the Pt-induced modulation could be a sum of several contributions.²⁴ For example, adducts located at crucial recognition sites during loading might lead to impaired functioning.^{25,26} Once loaded, the presence of a platinum-adduct in the biologically active guide strand might also interfere with the silencing ability by thermal destabilization of the duplex formed between the si- or miRNA and its complementary target mRNA.^{27–29}

To gain further insights into the endogenous response following *e.g.* clinical treatment with cisplatin, we present here an initial study illustrating a methodology that allows for documentation of the reactivity of cisplatin towards endogenous miRs. Since adduct profiles of nucleic acids are likely to be under kinetic rather than thermodynamic control,³⁰ we believe that such information serves as a guide to the identification of particularly reactive metal binding sites in the RNA environment. Towards this goal we here – to our knowledge for the first time – present data that allow for a comparison of the reactivity of model duplex RNAs (RNA-1 and RNA-2) with that of an endogenous mature miRNA (miR-146a), see Scheme 1. Highly reproducible kinetics were obtained using UV/vis spectroscopy, and allowed for the establishment of a reactivity trend of RNA-1 > miR-146a > RNA-2 at physiologically relevant salt concentrations.

Biochemistry and Structural Biology, KILU, Lund University, P.O. Box 124, SE-221 00 Lund, Sweden. E-mail: sofi.elmroth@biochemistry.lu.se; Fax: +46 46 222 4116; Tel: +46 46 222 3693

†Electronic supplementary information (ESI) available: Experimental details, thermal melting curves (Fig. S1), kinetic traces (Fig. S2 and S3), and observed pseudo-first-order rate constants as a function of [1a] (Fig. S4). See DOI: 10.1039/c3dt51788h





Scheme 1 RNA oligonucleotides used in the present study. Tentative G-N7 binding sites are underlined and the seed sequence of miR-146a is shown in italics.

As can be seen in Scheme 1, the fully complementary 15-mer RNAs both contain a single, centrally located preferred platination site³¹ in one of the strands: the r(GG)- or r(GUG)-sequence in RNA-1 and RNA-2, respectively. Both these duplexes have recently been characterized with respect to thermodynamic properties and the effects of cisplatin binding.³² At the salt concentrations investigated, these RNAs have similar melting temperatures, see Table 1, *ca.* 47 and 60 °C at $C_{\text{Na}^+} = 29$ and 129 mM, respectively. Further, platination leads to significant duplex destabilization, with a reduction of T_m by *ca.* 10 °C for RNA-1 and 18 °C for RNA-2.³² Based on these observations, we have speculated that when subjected to cisplatin at a temperature just below the melting point, the

expected metal-induced melting of these duplexes could be used to directly monitor the rate of platinum binding. An example of the spectral changes on addition of **1a** to RNA-1 is shown in Fig. 1A. As can be seen here, platinum exposure leads to an increase in absorbance of *ca.* 0.10 a.u. at $\lambda = 260$ nm. The absorbance changes are, for all RNA-duplexes, in good agreement with the ΔA -value that can be expected to be obtained by subtracting the absorbance value at $\lambda = 260$ nm obtained at 38 °C from that of the plateau-region obtained after melting the same RNA³³ (compare Fig. S1–S3†), thus supporting the mechanism suggested above. Further, inspection of the spectra as a function of time, here illustrated every 200th minute, shows a time dependent and gradual increase of absorbance and a small, but significant change from a maximum at λ *ca.* 258 nm to a maximum at λ *ca.* 260 nm, in accordance with the hyperchromicity and bathochromic shift expected following nucleic acid duplex melting.³⁴

For a mechanism involving a direct reaction between **1a** and the RNA duplex as the rate determining step, the rate of conversion of reactants to products should obey first-order dependence on the concentration of both **1a** and the target RNA: $\nu = k_{2,\text{app}}[\mathbf{1a}][\text{RNA}_{\text{duplex}}]$.³¹ Further, under pseudo-first-order conditions with $[\mathbf{1a}] \gg [\text{RNA}_{\text{duplex}}]$, the observed rate constant should be linearly dependent on $[\mathbf{1a}]$, and the time dependence can be well described by an exponential function of the type: $y = A \exp(-k_{\text{obs}}t) + B$, where $k_{\text{obs}} = k_{2,\text{app}}[\mathbf{1a}]$. To test the latter hypothesis, a series of experiments were next

Table 1 Summary of melting temperatures (T_m) and reaction rate constants (k_{obs} and $k_{2,\text{app}}$) for RNA-1, RNA-2 and miR-146a^a

Duplex	T_m^b (°C)	$10^4 \times k_{\text{obs}}$ (s ⁻¹)					$k_{2,\text{app}}^c$ (M ⁻¹ s ⁻¹)
		C_{Pt} (μM) 7.5	C_{Pt} (μM) 15.0	C_{Pt} (μM) 22.5	C_{Pt} (μM) 30.0	C_{Pt} (μM) 45.0	
$C_{\text{Na}^+} = 29$ mM							
RNA-1	47.8 ± 0.3	1.9	5.0	6.9	8.6	10	22.1 ± 1.7
RNA-2	47.4 ± 0.1	1.6	4.3	5.8	7.3	9.4	20.1 ± 1.1
miR-146a	37.3 ± 0.2	2.2	4.0	5.8	7.2	9.9	20.4 ± 0.6
$C_{\text{Na}^+} = 129$ mM							
RNA-1	60.4 ± 0.1	0.54	1.6	2.2	2.7	3.5	7.72 ± 0.45
RNA-2	60.1 ± 0.2	0.39	0.66	0.90	1.2	1.7	3.54 ± 0.04
miR-146a	50.4 ± 0.1	0.50	0.83	1.2	1.5	2.2	4.51 ± 0.10

^a Measurements were conducted with an individual RNA strand concentration of 1.5 μM, resulting in a total strand concentration ($C_{\text{T,RNA}}$) of 3.0 μM. ^b Measurements performed in triplicates. ^c Indicated errors correspond to the standard error.

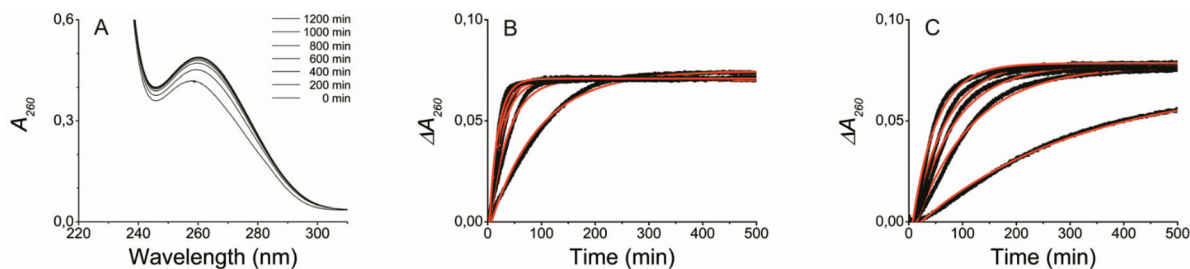


Fig. 1 Spectral changes as a function of time and related kinetic traces together with fits to an exponential function obtained after addition of **1a** to RNA-1 in buffered solution at 38 °C. (A) $C_{\mathbf{1a}} = 7.5$ μM, $C_{\text{T,RNA-1}} = 3.0$ μM, $C_{\text{Na}^+} = 129$ mM, and pH = 5.7, (B) $C_{\mathbf{1a}} = 7.5, 15.0, 22.5, 30.0$ and 45.0 μM, $C_{\text{T,RNA-1}} = 3.0$ μM, $C_{\text{Na}^+} = 29$ mM, and pH = 5.8, (C) $C_{\mathbf{1a}} = 7.5, 15.0, 22.5, 30.0$ and 45.0 μM, $C_{\text{T,RNA-1}} = 3.0$ μM, $C_{\text{Na}^+} = 129$ mM, and pH = 5.7.



conducted in which the absorbance change at $\lambda = 260$ nm was followed as a function of time. The reaction was studied at two different salt concentrations, at $C_{\text{Na}^+} = 29$ and 129 mM, with increasing concentrations of **1a** in the interval 7.5–45.0 μM . The resulting experimental data obtained after exposure of RNA-1 to **1a**, together with a fit of data to single exponential functions, are illustrated in Fig. 1B and 1C (see Fig. S2 and S3† for the corresponding data for RNA-2 and miR-146a). As can be seen here, the nature of the absorbance change is clearly dependent on the concentration of added **1a**, and also well described by an exponential function under all investigated reaction conditions. The present kinetic data are thus indicative of the formation of a mono-platinated duplex as the step initiating melting.³⁵ Further, a visual comparison of the 1st half-life for similar platinum concentrations shows that the reaction is salt dependent, with a pronounced higher reactivity at the lower salt concentration employed. For example, $t_{1/2}$ increases from ca. 90 to 250 min with a change of C_{Na^+} from 29 to 129 mM at the lowest platinum concentration employed: $[\mathbf{1a}] = 7.5 \mu\text{M}$, compare the bottom curves in Fig. 1B and 1C. This observation is in line with the expected behaviour of a system involving charge neutralization as the rate determining step, and of a magnitude similar to earlier reports on salt-dependent metalation kinetics.^{16,31} Further, for all RNA duplexes, a linear relationship between k_{obs} and $[\mathbf{1a}]$ was observed, thus allowing for determination of $k_{2,\text{app}}$ directly from the slope (see Fig. S4† for an illustration of data obtained for RNA-1, RNA-2 and miR-146a). The obtained values for k_{obs} and $k_{2,\text{app}}$ are summarized in Table 1. The data reveal that the three target RNAs studied here have similar reactivity at the lower salt concentration employed, with $k_{2,\text{app}}$ ca. $20 \text{ M}^{-1} \text{ s}^{-1}$, with only a slight tendency for a higher reactivity of the GG-containing RNA-1 ($k_{2,\text{app}} = 22.1 \pm 1.7 \text{ M}^{-1} \text{ s}^{-1}$). At the higher salt concentration however, the reactivity varies significantly between the duplexes, revealing RNA-1 to be the most reactive one, with $k_{2,\text{app}}$ ca. $7.7 \text{ M}^{-1} \text{ s}^{-1}$, followed in reactivity by miR-146a ($k_{2,\text{app}}$ ca. $4.5 \text{ M}^{-1} \text{ s}^{-1}$) and RNA-2 ($k_{2,\text{app}}$ ca. $3.5 \text{ M}^{-1} \text{ s}^{-1}$). The latter data thus seem to suggest that the monoaquated form of cisplatin is able to discriminate between RNA target sites at the salt concentrations relevant for biological systems. The sequence of reactivity obtained in the present investigation suggests an order according to: $k_{2,\text{app}}(\text{GG}) > k_{2,\text{app}}(\text{GUG})$, with centrally located consecutive GGs as the most reactive site.

Conclusions

In summary, we have presented here a method allowing for direct monitoring of metal binding to duplex RNA. The method relies on the ability of the monoaquated version of cisplatin (**1a**) to initiate duplex melting, and was applied here to two fully complementary 15-mer model RNAs and a mature version of the endogenous miR-146a. The reactivity trends reveal the miR to be as reactive as the model RNAs, indicating a half-life for interaction with **1a** in the hour-range at physiologically relevant salt concentrations.

Acknowledgements

Financial support from Cancerfonden (grant no. 110395), FLÅK-Forskarskolan i Läkemedelsvetenskap at Lund University, the Royal Physiographic Society, and the Crafoord Foundation is gratefully acknowledged.

Notes and references

- 1 A. P. Aalto and A. E. Pasquinelli, *Curr. Opin. Cell Biol.*, 2012, **24**, 333–340.
- 2 J. F. Kugel and J. A. Goodrich, *Trends Biochem. Sci.*, 2012, **37**, 144–151.
- 3 S. Memczak, M. Jens, A. Elefsinioti, F. Torti, J. Krueger, A. Rybak, L. Maier, S. D. Mackowiak, L. H. Gregersen, M. Munschauer, A. Loewer, U. Ziebold, M. Landthaler, C. Kocks, F. le Noble and N. Rajewsky, *Nature*, 2013, **495**, 333–338.
- 4 S. L. Ameres, J. Martinez and R. Schroeder, *Cell*, 2007, **130**, 101–112.
- 5 D. Baek, J. Villen, C. Shin, F. D. Camargo, S. P. Gygi and D. P. Bartel, *Nature*, 2008, **455**, 64–U38.
- 6 T. Kawamata and Y. Tomari, *Trends Biochem. Sci.*, 2010, **35**, 368–376.
- 7 Y. Shi and Y. Jin, *Sci. China Ser. C-Life Sci.*, 2009, **52**, 205–211.
- 8 S. Volinia, G. A. Calin, C. G. Liu, S. Ambs, A. Cimmino, F. Petrocca, R. Visone, M. Iorio, C. Roldo, M. Ferracin, R. L. Prueitt, N. Yanaihara, G. Lanza, A. Scarpa, A. Vecchione, M. Negrini, C. C. Harris and C. M. Croce, *Proc. Natl. Acad. Sci. U. S. A.*, 2006, **103**, 2257–2261.
- 9 G. A. Calin and C. M. Croce, *Nat. Rev. Cancer*, 2006, **6**, 857–866.
- 10 P. Kantharidis, B. Wang, R. M. Carew and H. Y. Lan, *Diabetes*, 2011, **60**, 1832–1837.
- 11 A. Lujambio and S. W. Lowe, *Nature*, 2012, **482**, 347–355.
- 12 L. Kelland, *Nat. Rev. Cancer*, 2007, **7**, 573–584.
- 13 D. Wang and S. J. Lippard, *Nat. Rev. Drug Discovery*, 2005, **4**, 307–320.
- 14 J. M. Pascoe and J. J. Roberts, *Biochem. Pharmacol.*, 1974, **23**, 1345–1357.
- 15 M. Akaboshi, K. Kawai, H. Maki, K. Akuta, Y. Ujeno and T. Miyahara, *Jpn. J. Cancer Res.*, 1992, **83**, 522–526.
- 16 M. Hägerlöf, P. Papsai, C. S. Chow and S. K. C. Elmroth, *J. Biol. Inorg. Chem.*, 2006, **11**, 974–990.
- 17 K. Rijal and C. S. Chow, *Chem. Commun.*, 2009, 107–109.
- 18 A. A. Hostetter, M. F. Osborn and V. J. DeRose, *ACS Chem. Biol.*, 2012, **7**, 218–225.
- 19 J. S. Parker, *Silence*, 2010, **1**(3), 1–10.
- 20 G. Sun, J. Yan, K. Noltner, J. Feng, H. Li, D. A. Sarkis, S. S. Sommer and J. J. Rossi, *RNA-Publ. RNA Soc.*, 2009, **15**, 1640–1651.
- 21 M. Hägerlöf, H. Hedman and S. K. C. Elmroth, *Biochem. Biophys. Res. Commun.*, 2007, **361**, 14–19.



- 22 A. S. Snygg and S. K. C. Elmroth, *Biochem. Biophys. Res. Commun.*, 2009, **379**, 186–190.
- 23 H. K. Hedman, F. Kirpekar and S. K. C. Elmroth, *J. Am. Chem. Soc.*, 2011, **133**, 11977–11984.
- 24 A. Reynolds, D. Leake, Q. Boese, S. Scaringe, W. S. Marshall and A. Khvorova, *Nat. Biotechnol.*, 2004, **22**, 326–330.
- 25 J. W. Gaynor, B. J. Campbell and R. Cosstick, *Chem. Soc. Rev.*, 2010, **39**, 4169–4184.
- 26 J. C. Henry, A. C. P. Azevedo-Pouly and T. D. Schmittgen, *Pharm. Res.*, 2011, **28**, 3030–3042.
- 27 Q. Du, H. Thonberg, J. Wang, C. Wahlestedt and Z. C. Liang, *Nucleic Acids Res.*, 2005, **33**, 1671–1677.
- 28 N. S. Petrova, M. I. Meschaninova, A. G. Venyaminova, M. A. Zenkova, V. V. Vlassov and E. L. Chernolovskaya, *FEBS Lett.*, 2011, **585**, 2352–2356.
- 29 J. W. Engels, *New Biotechnol.*, 2013, **30**, 302–307.
- 30 E. G. Chapman, A. A. Hostetter, M. F. Osborn, A. L. Miller and V. J. DeRose, *Met. Ions Life Sci.*, 2011, **9**, 347–377.
- 31 A. S. Snygg, M. Brindell, G. Stochel and S. K. C. Elmroth, *Dalton Trans.*, 2005, 1221–1227.
- 32 C. Polonyi, I. Albertsson, M. S. Damian and S. K. C. Elmroth, *Z. Anorg. Allg. Chem.*, 2013, **639**, 1655–1660.
- 33 For RNA-1, RNA-2 and miR-146a at $C_{\text{Na}^+} = 129$ mM the absorbance change is due to conversion of predominantly duplex RNA to single-stranded oligonucleotides. For miR-146a at $C_{\text{Na}^+} = 29$ mM, the reacting RNA-pool is a mixture of duplex- and corresponding single-stranded material thus resulting in a reduction of the measured ΔA -value by ca. 50%.
- 34 V. A. Bloomfield, D. A. Crothers and I. Tinoco Jr., *Nucleic Acids: Structures, Properties, and Functions*, University Science Books, Sausalito, CA, 2000.
- 35 Characterization of adduct type(s) is currently ongoing in our laboratory, C. Polonyi and S. K. C. Elmroth, *private communication*.

